On the advanced microstructural characterisation of additively manufactured alumina-zirconia based eutectic ceramics: Overview and outlook

Mainak Saha[1],[2]

[1]Department of Metallurgical and Materials Engineering, Indian Institute of Technology Madras, Chennai-600036

[2]Department of Metallurgical and Materials Engineering, National Institute of Technology Durgapur-713209

Corresponding authors: Mainak Saha

Email address: mainaksaha1995@gmail.com

Phone number: +918017457062/+919434789014

ORCID: Mainak Saha: 0000-0001-8979-457x

Abstract

Recently, there have been a number of reports on the fabrication of Alumina-Zirconia (Al_2O_3-ZrO_2 (AZ))-based eutectic ceramics using laser additive manufacturing (AM) techniques owing to the exceptional creep and oxidation resistance coupled with excellent microstructural stability in these materials. Moreover, a number of interesting microstructural features (in these materials) have been reported to be formed by the variation of process parameters (especially, laser scanning speed) associated with the aforementioned AM techniques. The present review provides an overview of the present state of research in the area of laser AM AZ-based eutectic ceramics and highlights the challenges and future outlooks in this avenue of research. In addition, the requirement of employing correlative microstructural characterisation in these materials has been highlighted in the outlooks section.

Keywords: Al_2O_3-based eutectic ceramics, Additive Manufacturing

Introduction

Alumina (Al_2O_3)-based ceramics find extensive industrial applications owing to a number of desirable properties which mainly include low density, high compressive strength, wear resistance, and electrical and thermal insulation properties [1]. A combination of good compressive properties of high-purity Al_2O_3 along with biocompatibility makes Al_2O_3 ceramic a potential candidate for dental and orthopaedic applications [2]. On the other hand, laser additive manufacturing (AM) techniques (especially laser AM techniques) are based on a layer by layer deposition of materials, which leads to a large-scale microstructural heterogeneity and formation of cracks (due to thermal stresses) in the deposited layers [3]–[5]. However, for the aforementioned AM techniques, the material (to be deposited) needs to possess a good fracture toughness so that it does not fracture due to the formation of cracks during the layerwise deposition [3], [6]–[9]. The main limitation of Al_2O_3 ceramics is the low fracture toughness which restricts the application of laser-based AM techniques in these ceramics [1].

Adding Zirconia (ZrO_2) to Al_2O_3 ceramics has been reported to be an effective way of improving fracture toughness (in AM-based samples) through crack bridging and deflection mechanisms. Pappas et al. [1] have reported the influence of ZrO_2 addition to AM-based Al_2O_3 using laser direct deposition technique. Li and Zhang [10] have investigated the microstructure of Al_2O_3-ZrO_2 (AZ) ceramics fabricated using laser direct deposition technique with ZrO_2 content >35 wt.%. Wilkes et al. [11] have reported that preheating of every layer (using a CO_2 laser beam) may be successfully employed to eliminate micro-cracking in AZ ceramics. Homeny and Nick [12] have investigated the structure-property correlation in AZ-Y_2O_3 eutectic ceramic. Moreno and Yoshimura [13] have investigated the stabilisation of ZrO_2 lamella in rapidly solidified AZ eutectic ceramic. Trnovcova et al. [14] have investigated the microstructure and physical properties of directionally solidified AZ eutectic ceramic. The present review is aimed at providing an overview of the present state of research in the field of laser AM AZ-based eutectic ceramics by highlighting three recent investigations in the particular avenue. In addition, a future outlook in this avenue has also been briefly highlighted towards the end of the review.

1. Characterisation of colonial boundaries in AZ-GdAlO₃ eutectic ceramic fabricated using laser directed energy deposition

Liu et al. [15] have investigated the microstructure of AZ-$GdAlO_3$ eutectic ceramic fabricated using laser directed energy deposition (LDED) technique. The formation of periodic banded structures was reported along the building direction (BD) and its formation was attributed to the abnormal growth of nanoscale features adjacent to the melt pool [15]. Within a eutectic colony, a "Chinese-script" eutectic structure with an entanglement of bright ($GdAlO_3$) and dark phases (Al_2O_3) was observed [15]. In addition, it was observed that colonies along the longitudinal section show a columnar morphology and are elongated perpendicular to the BD [15]. The aforementioned morphology of the colonies (along the longitudinal section) was mainly attributed to the heat conduction behaviour in the melt pool due to which the microstructural growth occurs against heat flow direction leading to an elongation of eutectic colonies (along the longitudinal section) perpendicular to the melt pool [15]. Moreover, the eutectic spacing was reported to decrease from ~ 0.63 ± 0.11 μm at the sample surface to ~ 0.99 ± 0.08 μm at the centre of the sample [15]. This has been attributed to a higher cooling rate at the surface as compared to that of the sample interior [15]. **Fig. 1(a)** shows concave bands along BD. **Figs. 1(b-d)** show the Scanning Electron Microscopy (SEM)-based microstructures in the different layers of the cladding layer with colonial boundaries clearly visible.
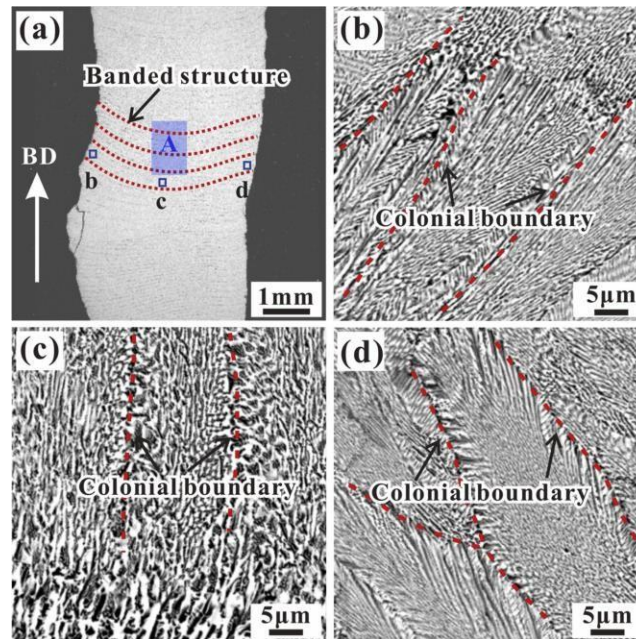
Fig. 1 SEM micrographs (of the longitudinal section) of the AZ-GdAlO$_3$ eutectic ceramic: **(a)** periodic banded structure, **(b)** Left side of a deposited layer, **(c)** Centre of a deposited layer, and **(d)** Right side of a deposited layer [15].

3. Microstructure obtained during solidification of selective laser melted AZ-GdAlO$_3$ eutectic ceramic

Liu et al. [16] have investigated the influence of laser scanning speed on the solidification of AZ-GdAlO$_3$ eutectic ceramic during selective laser melting (SLM) technique. The relative density of the solidified samples was reported to decrease from 98.7% to 95.7% with increasing laser scanning speed to ~48 mm/min [16]. In addition, it was observed that the primary heat transfer mechanism associated with the solidification phenomenon is thermal conduction due to which there was a decrease in both melting width and depth with increase in scanning speed [16]. Interestingly, it was also observed that the eutectic spacing in the top zone of the melt pool initially decreases with increasing laser scanning speed from 6 mm/min till 12 mm/min and then increases with increasing scanning speed from 12 mm/min till 48 mm/min [16]. The aforementioned trend in the eutectic spacing with scanning speed was attributed to a change in solidification rate controlling factor from laser scanning speed to the angle between the scanning direction and the growth direction of the microstructure [9], [16]. Quenching induced micro-cracks and increased surface roughness (due to bailing effect and presence of microstructural pores) were reported for scanning speeds of <12 mm/min [16]. Moreover, solidification defects were reported to be minimised for laser scanning speed of ~12 mm/min [16].

4. Nanostructured AZ-YAG fabricated using laser engineered net shaping technique

Fan et al. [17] have reported the fabrication of highly dense ($\geq$ 98%) thin-walled Al$_2$O$_3$-YAG-ZrO$_2$ (AYZ) eutectic ceramic using LENS technique. The as-synthesized state of the material shows a cellular microstructure with the interpenetration of three phases (namely, α-Al$_2$O$_3$,

YAG and ZrO_2) [17]. In addition, a morphological transition from planar to cellular eutectic microstructure (along BD) was reported for every deposited layer [17]. **Fig. 2(a)** shows a scanning transmission electron microscopy (STEM)-high-angle annular dark field (HAADF) image of AYZ ceramic in as-fabricated condition [17]. **Figs. 2(b-e)** shows the corresponding STEM-Energy Dispersive Spectroscopy (EDS) maps for different elements: Al, Y, Zr and O. The dark, grey and bright phases in STEM-HAADF image (**Fig. 2(a)**) correspond to α-Al_2O_3, YAG and cubic ZrO_2 phases respectively, as is also evident from **Figs. 2(b-e)** and **Table. 1** [17]. Besides, from **Figs. 2(c-e)** and **Table. 1,** it may be observed that ~18 mol.% Y_2O_3 is dissolved in ZrO_2 in as-fabricated condition indicating that cubic ZrO_2 is stabilised by Y^{3+} during cooling and solidification (during LENS) [17].
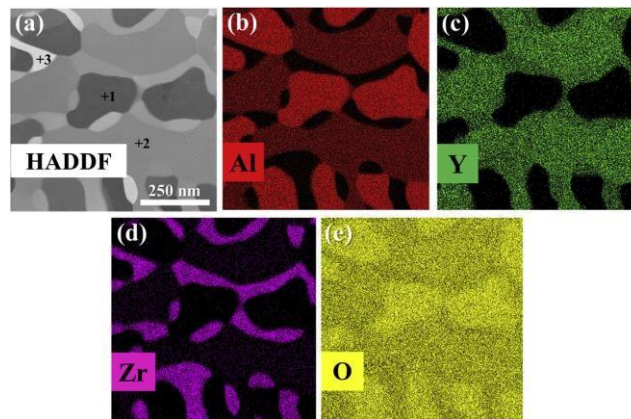

Fig. 2 AYZ: **(a)** STEM-HAADF image, and corresponding STEM-EDS maps of **(b)** Al, **(c)** Y, **(d)** Zr, and **(e)** O [17]. Points 1, 2 and 3 marked in part **(a)** represent the regions where point EDS mapping has been performed. Results of point EDS mapping at points 1, 2 and 3 have been shown in **Table. 1**

Table. 1 Composition (in at.%) at points 1, 2 and 3 obtained using point STEM-EDS analysis [17]

Elements	1	2	3
Al	35	22.5	1.3
Y	0	8.4	7.9
Zr	0	0.6	17.1
O	65	68.5	73.7

An irregular interpenetration of fibrous eutectic structure was also reported to occur along the boundary region of the fabricated specimens [17]. This was attributed to a much higher rate of solidification at the boundary region as compared to that within the sample interior [17]. In addition, the orientation relation between the three phases at the interior of LENSed samples was obtained as $<0001>_{Al2O3}$ // $<001>_{YAG}$ // $<001>_{ZrO2}$ (with a slight deviation of ~3.5° between $\{001\}_{YAG}$ with $\{11\text{-}20\}_{Al2O3}$ and $\{001\}_{ZrO2}$ obtained using Transmission Kikuchi Diffraction (TKD) technique and verified with High-resolution Transmission Electron

Microscopy (HRTEM) imaging of a triple junction formed between Al_2O_3, YAG and ZrO_2 phases (**Fig. 3**) [17]. The aforementioned deviation may be attributed to a competitive effect between interfacial energy and growth kinetics [17]. For instance, the lower interfacial energy of Al_2O_3/ZrO_2 interface (~ 0.74 J/m^2) as compared to that for Al_2O_3/YAG interface with an interfacial energy ~3.23 J/m^2 [17] may be attributed to a better parallel nature of $\{11\text{-}20\}$ $_{Al2O3}$ $//\{001\}$ $_{ZrO2}$ when compared with that for $\{11\text{-}20\}$ $_{Al2O3}//\{001\}$ $_{YAG}$ [9], [17].
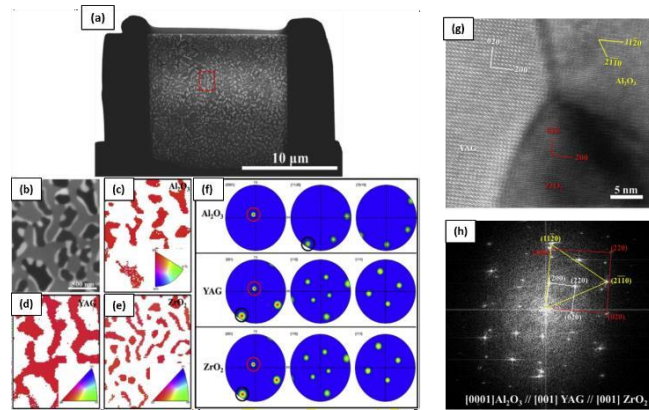

Fig. 3 AYZ: **(a)** SEM image of the electron transparent lamella of the transverse section of the LENSed specimen prepared using Focussed ion beam (FIB)-based liftout technique, **(b)** SEM image of region of interest for TKD mapping inside the cellular eutectic, **(c), (d),** and **(e)** TKD-based inverse pole figure (IPF) maps of Al_2O_3, YAG and ZrO_2 respectively, **(f)** Pole figures for the three constituent phases: Al_2O_3, YAG and ZrO_2 corresponding to **(c), (d)** and **(e)** respectively, **(g)** High-resolution Transmission Electron Microscope (HRTEM) micrograph of the transverse section showing a triple junction between Al_2O_3, YAG and ZrO_2 phases, and **(h)** Fast Fourier Transformation (FFT) diffraction pattern corresponding to part **(a)** with zone axis: $[0001]_{Al2O3}$ // $[001]_{YAG}$ // $[001]_{ZrO2}$ [17]. A magnified view of the region highlighted using a red-dotted rectangle in part **(a)** has been shown in part **(b)**.

Fig. 4 shows an SEM image of the longitudinal section of LENSed AYZ specimen subjected to TKD analysis along BD [17]. The growth direction of the cellular eutectics remains the same as that for the transverse section of AYZ samples i.e. $<0001>_{Al2O3}$ // $<001>_{YAG}$ // $<001>_{ZrO2}$ [17]. However, unlike the transverse section, the longitudinal section also shows YAG crystals with minor growth direction as $<111>$ [17]. This may be attributed to the deviation of these crystals (present mainly near cellular boundaries as shown in **Fig. 4**) from their habit planes and subsequent heading towards cellular boundary instead of remaining parallel with the cell growth direction. A similar observation has been reported for Al_2O_3-ZrO_2 cellular eutectic by Sayir and Farmer [18] and for Ni-Al-V eutectic alloys by Milenkovic et al. [19].
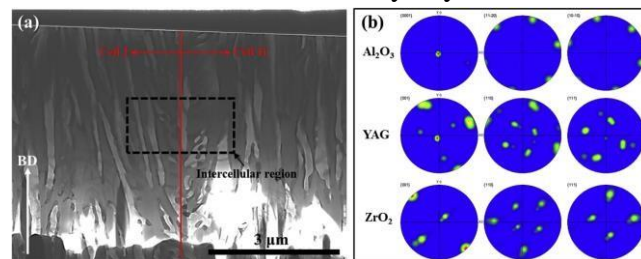
Fig. 4 AYZ: **(a)** SEM image of the electron transparent lamella of the longitudinal section of the LENSed specimen prepared using Focussed ion beam (FIB)-based liftout technique, TKD-based **(b)** pole figures of α-Al$_2$O$_3$, YAG and ZrO$_2$ [17]. Pole figures in part **(b)** have been obtained from the inter-cellular region enclosed with a block-dotted rectangular box in part **(a)**. In part **(a)**, BD abbreviates for building direction.

5. Summary and outlook

In the present review, the present state of research in the field of laser AM-based AZ ceramics has been briefly highlighted. The present focus (in this avenue) is to engineer the microstructure (based on optimising a number of process parameters associated with AM-based fabrication techniques) to render these ceramics superior in terms of mechanical properties compared to those fabricated using conventional techniques. However, in the context of eutectic ceramics (including AZ ceramics), characterisation of the different interfaces (mostly, the eutectic boundaries, in the present context) has not been addressed till date. For instance, in the context of laser AM-based AZ ceramics, the case study discussed in **section 4** is the only work (till date) which has been successfully able to use FIB-based liftout technique for obtaining electron transparent lamella from both transverse and longitudinal sections in AYZ ceramic in order to determine the orientation relationship between the individual phases (α-Al$_2$O$_3$, YAG and ZrO$_2$) using TKD technique.

In the last four decades, grain boundary engineering (GBE) of both metallic materials and ceramics has evolved as a methodology to optimise the different properties of these materials based on replacing high-energy random high-angle GBs (HAGBs) with low-energy GBs [20], [21]. Particularly, in the context of metallic materials with mostly cubic crystal structures, GBE has been defined as a methodology to replace HAGBs with special HAGBs (with low-energy) also known as Coincidence Site Lattice (CSL) boundaries [22]–[25]. The entire methodology of GBE is based on reducing the overall GB energy in a microstructure so as to make the 2D interfaces (GBs and IBs) resistant to corrosion, oxidation, abnormal grain growth and intergranular fracture. Moreover, the most common method to obtain GBE microstructures in most metallic materials is thermo-mechanical processing (TMP) [26]. In the context of ceramics with more complex crystal structures, CSL theory fails and hence, the existence of low-energy CSL boundaries is hard to visualise [27]–[29]. Furthermore, the techniques used (especially TMP) to obtain GBE microstructures in metallic materials cannot be used in ceramics owing to their low deformability both at room and elevated temperatures. Hence, there lies a huge challenge in obtaining GBE microstructures in AZ ceramics. This also paves a new avenue of research in the context of AZ ceramics. In addition, one of the most recently evolved methodologies towards correlating the structure of GBs and interphase boundaries (IBs) with their local atomic-scale composition (in polycrystalline materials) is Correlative Microscopy [30], [31]. Particularly, in the context of metallic materials, this methodology has been extensively used to study both the structure and composition of GBs and also to address the five macroscopic and three microscopic degrees of freedom (DOFs) (of GBs and IBs). However, in the context of AZ ceramics, there is hardly any correlative microstructural investigation till date. This may be attributed to the complexity associated with crystal structures and sample preparation. Moreover, as mentioned in **section 1**, laser AM-based techniques are based on layer-by-layer deposition of materials. This adds up to the complexity (in terms of obtaining GBE microstructures) by inducing large-scale microstructural

heterogeneities (with high defect concentration) [32-41], resulting in non-equilibrium microstructures. Hence, obtaining GBE microstructures in AM-based AZ ceramics provides an immense potential towards future investigations in field of AZ ceramics.

Acknowledgement

References

[1]   J. M. Pappas, A. R. Thakur, and X. Dong, "Effects of zirconia doping on additively manufactured alumina ceramics by laser direct deposition," *Materials and Design*, vol. 192, p. 108711, Jul. 2020, doi: 10.1016/j.matdes.2020.108711.

[2]   V. K. Balla, S. Bose, and A. Bandyopadhyay, "Processing of bulk alumina ceramics using laser engineered net shaping," *International Journal of Applied Ceramic Technology*, vol. 5, no. 3, pp. 234–242, May 2008, doi: 10.1111/j.1744-7402.2008.02202.x.

[3]   C. K. Chua, K. F. Leong, and J. An, "Additive Manufacturing and 3D Printing," in *Biomedical Materials*, Springer International Publishing, 2021, pp. 621–652. doi: 10.1007/978-3-030-49206-9_19.

[4]   O. Abdulhameed, A. Al-Ahmari, W. Ameen, and S. H. Mian, "Additive manufacturing: Challenges, trends, and applications," *Advances in Mechanical Engineering*, vol. 11, no. 2, Feb. 2019, doi: 10.1177/1687814018822880.

[5]   B. Durakovic, "Design for additive manufacturing: Benefits, trends and challenges," *Periodicals of Engineering and Natural Sciences*, vol. 6, no. 2, pp. 179–191, Dec. 2018, doi: 10.21533/pen.v6i2.224.

[6]   W. E. Frazier, "Metal additive manufacturing: A review," *Journal of Materials Engineering and Performance*, vol. 23, no. 6. Springer New York LLC, pp. 1917–1928, 2014. doi: 10.1007/s11665-014-0958-z.

[7]   A. Zocca, P. Colombo, C. M. Gomes, and J. Günster, "Additive Manufacturing of Ceramics: Issues, Potentialities, and Opportunities," *Journal of the American Ceramic Society*, vol. 98, no. 7, pp. 1983–2001, Jul. 2015, doi: 10.1111/jace.13700.

[8]   A. Vyatskikh, S. Delalande, A. Kudo, X. Zhang, C. M. Portela, and J. R. Greer, "Additive manufacturing of 3D nano-architected metals," *Nature Communications*, vol. 9, no. 1, pp. 1–8, Dec. 2018, doi: 10.1038/s41467-018-03071-9.

[9]   M. Saha and M. Mallik, "Additive manufacturing of ceramics and cermets: present status and future perspectives," *Sādhanā 2021 46:3*, vol. 46, no. 3, pp. 1–35, Aug. 2021, doi: 10.1007/S12046-021-01685-2.

[10]   F. Li and Y. Zhang, " Microstructural characterization of Al 2 O 3 -ZrO 2 ceramic by laser direct material deposition ," *Journal of Laser Applications*, vol. 31, no. 2, p. 022509, May 2019, doi: 10.2351/1.5096125.

[11]   J. Wilkes, Y. C. Hagedorn, W. Meiners, and K. Wissenbach, "Additive manufacturing of ZrO2-Al2O3 ceramic components by selective laser melting," *Rapid Prototyping Journal*, vol. 19, no. 1, pp. 51–57, 2013, doi: 10.1108/13552541311292736.

[12]   J. Homeny and J. J. Nick, "Microstructure-property relations of alumina-zirconia eutectic ceramics," *Materials Science and Engineering A*, vol. 127, no. 1, pp. 123–133, Jul. 1990, doi: 10.1016/0921-5093(90)90198-C.

[13]   J. M. Calderon-Moreno and M. Yoshimura, "Stabilization of zirconia lamellae in rapidly solidified alumina-zirconia eutectic composites," *Journal of the European Ceramic Society*, vol. 25, no. 8 SPEC. ISS., pp. 1369–1372, Jan. 2005, doi: 10.1016/j.jeurceramsoc.2005.01.013.

[14]   V. Trnovcovfi, M. Starostin, V. Labas, and R. Cicka, "Microstructure and Physical Properties of Directionally Solidified Alumina-Zirconia Eutectic Composites," 1998.

[15]   H. Liu *et al.*, "One-step additive manufacturing and microstructure evolution of melt-grown Al2O3/GdAlO3/ZrO2 eutectic ceramics by laser directed energy deposition," *Journal of the European Ceramic Society*, vol. 41, no. 6, pp. 3547–3558, Jun. 2021, doi: 10.1016/j.jeurceramsoc.2021.01.047.

[16]   H. Liu *et al.*, "Effect of scanning speed on the solidification process of Al2O3/GdAlO3/ZrO2 eutectic ceramics in a single track by selective laser melting," *Ceramics International*, vol. 45, no. 14, pp. 17252–17257, Oct. 2019, doi: 10.1016/j.ceramint.2019.05.281.

[17]   Z. Fan *et al.*, "Nanostructured Al 2 O 3 -YAG-ZrO 2 ternary eutectic components prepared by laser engineered net shaping," *Acta Materialia*, vol. 170, pp. 24–37, May 2019, doi: 10.1016/j.actamat.2019.03.020.

[18]   A. Sayir and S. C. Farmer, "Effect of the microstructure on mechanical properties of directionally solidified Al2O3/ZrO2(Y2O3) eutectic," *Acta Materialia*, vol. 48, no. 18–19, pp. 4691–4697, Dec. 2000, doi: 10.1016/S1359-6454(00)00259-7.

[19]   S. Milenkovic, A. A. Coelho, and R. Caram, "Directional solidification processing of eutectic alloys in the Ni-Al-V system," *Journal of Crystal Growth*, vol. 211, no. 1, pp. 485–490, Apr. 2000, doi: 10.1016/S0022-0248(99)00783-6.

[20]   D. Raabe *et al.*, "Grain boundary segregation engineering in metallic alloys: A pathway to the design of interfaces," *Current Opinion in Solid State and Materials Science*, vol. 18, no. 4, pp. 253–261, 2014, doi: 10.1016/j.cossms.2014.06.002.

[21]   Y. Ikuhara, "Grain boundary and interface structures in ceramics," *Journal of the Ceramic Society of Japan*, vol. 109, no. 1271. Ceramic Society of Japan, pp. S110–S120, Jul. 01, 2001. doi: 10.2109/jcersj.109.1271_S110.

[22]   A. D. Rollett, "Texture development dependence on grain boundary properties," in *Materials Science Forum*, 2002, vol. 408–412, no. I, pp. 251–256. doi: 10.4028/www.scientific.net/msf.408-412.251.

[23]   M. Winning and A. D. Rollett, "Transition between low and high angle grain boundaries," *Acta Materialia*, vol. 53, no. 10, pp. 2901–2907, Jun. 2005, doi: 10.1016/j.actamat.2005.03.005.

[24]   D. Brandon, "25 Year Perspective Defining grain boundaries: An historical perspective the development and limitations of coincident site lattice models," *Materials Science and*

Technology*, vol. 26, no. 7. pp. 762–773, Jul. 01, 2010. doi: 10.1179/026708310X12635619987989.

[25] D. G. Brandon, "The structure of high-angle grain boundaries," *Acta Metallurgica*, vol. 14, no. 11, pp. 1479–1484, 1966, doi: 10.1016/0001-6160(66)90168-4.

[26] W. M. Ashmawi and M. A. Zikry, "Prediction of grain-boundary interfacial mechanisms in polycrystalline materials," *Journal of Engineering Materials and Technology, Transactions of the ASME*, vol. 124, no. 1, pp. 88–96, 2002, doi: 10.1115/1.1421611.

[27] V. Y. Gertsman, A. P. Zhilyaev, and J. A. Szpunar, "Grain boundary misorientation distributions in monoclinic zirconia," *Modelling and Simulation in Materials Science and Engineering*, vol. 5, no. 1, pp. 35–52, Jan. 1997, doi: 10.1088/0965-0393/5/1/003.

[28] H. Grimmer, "Coincidence-site lattices," *Acta Crystallographica Section A*, vol. 32, no. 5, pp. 783–785, Sep. 1976, doi: 10.1107/S056773947601231X.

[29] A. P. Sutton, R. W. Balluffi, and V. Vitek, "On intrinsic secondary grain boundary dislocation arrays in high angle symmetrical tilt grain boundaries," *Scripta Metallurgica*, vol. 15, no. 9, pp. 989–994, 1981, doi: 10.1016/0036-9748(81)90240-4.

[30] Y. Toji, H. Matsuda, M. Herbig, P. P. Choi, and D. Raabe, "Atomic-scale analysis of carbon partitioning between martensite and austenite by atom probe tomography and correlative transmission electron microscopy," *Acta Materialia*, vol. 65, pp. 215–228, Feb. 2014, doi: 10.1016/j.actamat.2013.10.064.

[31] C. H. Liebscher *et al.*, "Tetragonal fcc-Fe induced by κ -carbide precipitates: Atomic scale insights from correlative electron microscopy, atom probe tomography, and density functional theory," *Physical Review Materials*, vol. 2, no. 2, pp. 1–6, 2018, doi: 10.1103/PhysRevMaterials.2.023804.

[32] M. Schwentenwein and J. Homa, "Additive manufacturing of dense alumina ceramics," *International Journal of Applied Ceramic Technology*, vol. 12, no. 1, pp. 1–7, Jan. 2015, doi: 10.1111/ijac.12319.

[33] Saha M. Grain boundary segregation in steels: Towards engineering the design of internal interfaces. arXiv preprint arXiv:2202.12971. 2022 Feb 5.

[34] Saha M. New frontiers in characterising ZrB $ _2 $-MoSi $ _2 $ ultra-high temperature ceramics. arXiv preprint arXiv:2202.11162. 2022 Feb 5.

[35] Saha M. Fly ash composites: A review. arXiv preprint arXiv:2202.11167. 2022 Feb 5.

[36] Mallik M, Saha M. Carbon-Based Nanocomposites: Processing, Electronic Properties and Applications. InCarbon Nanomaterial Electronics: Devices and Applications 2021 May 23 (pp. 97-122). Singapore: Springer Singapore.

[37] Saha M, Mallik M. Additive manufacturing and characterisation of biomedical materials. InAdvanced Materials for Biomechanical Applications 2022 May 30 (pp. 29-57). CRC Press.

[38] Saha M, Mallik M. Surface engineering of nanomaterials: Processing and applications. InSurface Engineering 2022 Sep 14 (pp. 95-119). CRC Press.

[39] Saha M. 3D printing of nanoceramics: Present status and future perspectives. arXiv preprint arXiv:2210.06948. 2022 Sep 1.

[40] Saha M, Mallik M. Metal-based conducive nano-inks: synthesis and characterization techniques. SMART MULTIFUNCTIONAL NANO-INKS. 2023:27.

[41]   Saha M. On the advanced microstructural characterisation of additively manufactured alumina-zirconia based eutectic ceramics: Overview and outlook.